University of Florence

CERM – Magnetic Resonance Center

International Doctorate in Structural Biology

Cycle XX (2005-2007)

SOLUTION STRUCTURE OF PROTEIN COMPLEXES

Ph.D. thesis of

Leonardo Tenori

Tutor	Coordinator
Prof. Ivano Bertini	Prof. Claudio Luchinat

S.S.D. CHIM/03

This thesis has been approved by the University of Florence,
the University of Frankfurt and the Utrecht University

Nothing shocks me.
I'm a scientist.
(*Henry Jones Junior)*

Est aurum et multitudo gemmarum
et vas pretiosum labia scientiae.
(Liber Proœrbiorum, 20:15)

E porterem con rivelazion somma
saper ch'all'altro somma.
(Corrado R. L. dei Toscani)

CONTENTS

SYNOPSIS

The interactions between proteins are important for many biological functions. For example, signals from the exterior of a cell are mediated to the inside of that cell by protein-protein interactions of the signalling molecules. This process, called signal transduction, plays a fundamental role in many biological processes and in many diseases (e.g. cancer). Proteins might interact for a long time to form part of a protein complex, a protein may be carrying another protein (for example, from cytoplasm to nucleus or vice versa), or a protein may interact transiently with another protein to modify it (for example, a protein kinase will add a phosphate to a target protein). This modification of proteins can itself change protein-protein interactions. For example, some proteins with SH2 domains only bind to other proteins when they are phosphorylated on the amino acid tyrosine.

A protein complex is a group of two or more associated proteins formed by protein-protein interaction that is stable over time. Protein complexes can be considered a form of quaternary structure. Understanding the functional interactions of proteins is an important research focus in biochemistry and cell biology.

Complex formation often serves to activate or inhibit one or more of the associated proteins.

Many protein complexes are established, particularly in the model organism *Saccharomyces cerevisiae*, a yeast.

The molecular structure of protein complexes and its dynamical properties can be determined by experimental techniques such as X-ray crystallography or nuclear magnetic resonance (NMR) spectroscopy. Increasingly, the theoretical option of protein-protein docking is also becoming available.

In conclusion, protein complexes interactions are of central importance for a significant part of all process in a living cell. Information about these interactions improves our understanding of diseases and can provide the basis for new therapeutic approaches.

The research group where I have attended my PhD course has a long experience in metalloproteins. I become part of this project studying some copper proteins that can form protein complexes (S100A13, CCC2, CopA) from a structural and dynamical point of view using NMR spectroscopy.

Human S100A13 is an ubiquitous protein of 98 aminoacids which represents one of the latest members identified in the S100 protein family. S100A13 is involved in the cellular export of interleukin (IL)-1α, a potent pro-inflammatory cytokine, and of fibroblast growth factor-1 (FGF-1), which plays a crucial role in angiogenesis and tissue regeneration. Export is based on the Cu^{II}-dependent formation of multiprotein complexes, containing the S100A13 protein, that assemble near the inner surface of the plasma membrane. With the aim of obtain more information on the mechanism of this complex formation we have solved the solution structure of the human S100A13 protein in the apo and in the calcium form.

Ccc2 is a multi-domain membrane protein, comprising a cytoplasmic tail containing two distinct soluble metal-binding domains, which are quite similar in sequence to one

another and are predicted to have the same fold (βαββαβ ferredoxin fold) as the partner protein Atx1. A long-standing open question is the role of the multiple cytosolic metal-binding domains in copper-transporting ATPases. Homologous ATPases even from phylogenetically close organisms display a variable number of such domains, with different fold stability and different capability of binding copper. Notably, other metal-transporting P-type ATPases such as the sarcoplasmic/endoplasmic reticulum calcium ATPase (SERCA) or the Na+ /K+ ATPase do not possess any cytoplasmic metal-binding domain. Various experiments based on the rescue of yeast variants where the ccc2 gene had been suppressed have shown that truncated variants of human ATP7A or ATP7B containing only two or even one soluble domain allow Δccc2 yeast to grow on an iron- and copper-limited medium at levels close to that of wild-type yeast. Another noteworthy feature is that in the ATPases containing multiple soluble metal-binding domains, the two closest in sequence to the transmembrane segments (i.e. the most C-terminal ones in the tail) are always closely spaced in sequence (four to less than 10 aminoacids), whereas the other domains, if any, are widely spaced in sequence, with the linker stretches spanning up to several tens of aminoacids. The two most C-terminal domains form a relatively compact unit, which is only loosely coupled, from a structural point of view, to the remainder of the tail. The organization of the two most C-terminal domains in the ATP7B protein prevents transfer of copper(I) from one domain to the other. Based on these observations, it has been proposed that in the proteins containing more than two domains, the cellular role of the additional domains is that of regulating protein trafficking be-tween the TGN and the plasma membrane. To obtain further insight into these complex systems, we have

undertaken an NMR investigation of the entire two-domain cytoplasmic tail of Ccc2 and of its interaction with copper(I) and with copper(I)-Atx1.

CopA is a 803 amino acid residue protein with eight predicted transmembrane segments and two N-terminal soluble domains (approximately residues 1 – 72 and 73 – 147) that each contains a conserved MXCXXC metal binding motif typically found in homologous P-type ATPases and copper chaperone proteins. These bear close resemblance in primary sequence to CopZ, and are involved in accepting Cu(I) from CopZ. The solution structure of the second N-terminal do-main of CopA (CopAb) was previously determined as a separate domain and as part of a two domain protein. These revealed almost identical ferredoxin-like, βαββαβ structures typical for this class of copper chaperone. CopAa, either separately or as part of CopAab, was previously found to be unstable, but could be stabilized through the introduction of a single substitution, Ser46Val, leading to structures of domain a, separately, and as part of CopAab, which also revealed a typical Atx1-like structure.

Now we have generated a wild-type form of B. subtilis CopAab that is sufficiently stable for structural analysis, and we report the solution structure of the apo-form of the protein, and a detailed spectroscopic and bioanalytical investigation of the Cu(I)-binding properties of the wild-type protein and its interaction with the partener CopZ.

CHAPTER 1

GENERAL INTRODUCTION

§ 1.1 STRUCTURAL INTERPLAY BETWEEN CALCIUM(II) AND COPPER(II) BINDING TO S100A13

THE ROLE OF CALCIUM IN BIOLOGICAL SYSTEMS

Calcium is a ubiquitous second messenger that regulates a diverse array of cellular events, including muscle contraction, neurotransmitter release, fertilization and cell growth. As a result of its pivotal role, the cellular machinery maintains tight control over the concentration of calcium, which ranges from resting levels near 100 nM to signalling levels near 1 μM. The influx of calcium from the extracellular matrix is controlled by voltage-gated or receptor-operated channels that respond to changes in membrane potential or activation via ligand binding. Calcium can also be sourced from the endoplasmic reticulum where the ion is passed to the cytoplasm by the ryanodine or inositol 1,4,5-trisphosphate receptors. Resting calcium levels are re-established by reciprocal mechanisms such as plasma membrane pumps or exchangers or through re-entry to the endoplasmic reticulum via Ca^{2+}-ATPases [1, 2]. The intermediary calcium pulse that results from competing influx

1 Berridge, M. J., Lipp, P. and Bootman, M. D. (2000) The versatility and universality of calcium signalling. *Nat. Rev. Mol. Cell Biol.* **1**, 11–21.

2 Berridge, M. J., Bootman, M. D. and Roderick, H. L. (2003) Calcium signalling: dynamics, homeostasis and remodelling. Nat. *Rev. Mol. Cell Biol.* **4**, 517–529.

and efflux of calcium stimulates a variety of cellular activities. The increased calcium level can act as a feedback inhibitor to switch the calcium import machinery off. Furthermore, the bulk of the intracellular calcium is absorbed by calcium-buffering proteins that have high capacities for calcium, tight binding affinities or unique kinetic properties that act to fine-tune the levels and availability of free cytosolic calcium.

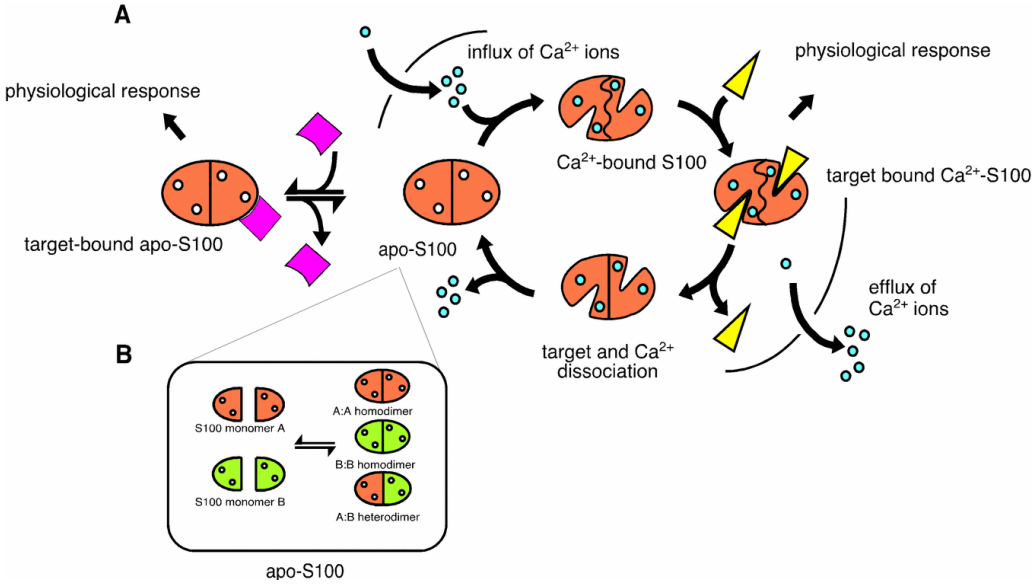

Figure 1
Calcium-dependent and -independent interactions of the S100 family.
(**A**) S100 proteins generate diverse physiological responses by interacting with target molecules (pink and yellow). At low calcium concentrations, S100 proteins (orange) reside in their calcium-free (apo) state. Upon influx of calcium via voltage-gated or receptor-mediated channels, the S100 protein binds calcium and undergoes a conformational change that modifies its hydrophobic surface properties. This allows the protein to interact with a wide spectrum of target proteins (yellow) to stimulate a physiological response. Release of calcium through Ca^{2+}-ATPase activity results in the dissociation of calcium and target protein from the S100 protein, returning it to its apo state. Although the majority of S100-target interactions are calcium-dependent, some S100 members have been shown to interact with target proteins (pink) in a calcium-independent fashion. (**B**) Dimeric S100 proteins can exchange subunits with other members of the S100 proteins to form homo- and hetero-dimers in the same cell type as shown by in vitro and in vivo experiments. The populations of each species are dependent on the concentration of the S100 protein in the cell and the relative affinities for the S100 homo- and hetero-dimers.

However, the most important events arising from the calcium signal are the triggering of downstream biological events modulated through binding of calcium to a

large number of calcium-sensor proteins (**Figure 1**). By far the largest group of sensors is the EF-hand calcium-binding proteins, of which more than 600 have been identified from the human genome.

EF-HAND CALCIUM-BINDING PROTEINS

Kretsinger and Nockolds [3] first identified the EF-hand motif, two α-helices with an intervening 12-residue calcium-binding loop, more than 30 years ago. Structural analysis indicates the chelating residues in the calcium-binding loop form a conserved pentagonal bipyramidal arrangement around the Ca^{2+} ion, utilizing the side chains at positions 1, 3, 5, 9 (via water) and 12 and backbone carbonyl group of position 7 [4]. Strong preferences exist for aspartate and glutamate in the 1 and 12 co-ordinating positions respectively, and glycine at the non-co-ordinating position 6 [5]. Functional EF-hands are found in pairs [6] and are required for the correct folding of the proteins and unique variations of calcium binding co-operativity.

The calcium signalling role for EF-hand proteins was first established for calmodulin through its activation of 3´,5´-cyclic nucleotide phosphodiesterase [7] and its

3 Kretsinger, R. H. and Nockolds, C. E. (1973) Carp muscle calcium-binding protein. II. Structure determination and general description. *J. Biol. Chem.* **248**, 3313–3326.

4 Strynadka, N. C. J. and James, M. N. G. (1989) Crystal structures of the helix–loop–helix calcium-binding proteins. *Annu. Rev. Biochem.* **58**, 951–998.

5 Marsden, B. J., Shaw, G. S. and Sykes, B. D. (1990) Calcium binding proteins: elucidating the contributions to calcium affinity from analysis of species variants and peptide fragments. *Biochem. Cell Biol.* **68**, 587–601.

6 Shaw, G. S., Hodges, R. S. and Sykes, B. D. (1990) Calcium-induced peptide association to form an intact protein domain: ^{1}H NMR structural evidence. *Science* **249**, 280–283.

7 Cheung, W. Y. (1970) Cyclic 3´,5´-nucleotide phosphodiesterase: demonstration of an activator. *Biochem. Biophys. Res. Commun.* **38**, 533–538.

ability to bind calcium [8]. Subsequently, the structural basis for calmodulin activation [9] showed a calcium-dependent rearrangement of its helices, resulting in the exposure of a hydrophobic surface used to recruit target proteins. A related calcium-sensitive mechanism exists for the muscle contractile EF-hand protein troponin-C [10, 11], where calcium-binding modulates its interactions with troponin-I within the muscle complex. More recently, it has been established that the S100 proteins comprise a complex grouping of EF-hand calcium-sensors that have diverse tissue distributions and many protein interactions that result in multiple physiological responses [12] (**Figure 1**). Interest in the S100 proteins has been sparked by their involvement in several human diseases, such as Alzheimer's disease, cancer and rheumatoid arthritis, usually due to modified levels of expression of the S100 members [13, 14].

8 Teo, T. S. and Wang, J. H. (1973) Mechanism of activation of a cyclic adenosine 3′:5′-monophosphate phosphodiesterase from bovine heart by calcium ions: identification of the protein activator as a Ca^{2+} binding protein. *J. Biol. Chem.* **248**, 5950–5955.

9 Ikura, M., Clore, G. M., Gronenborn, A. M., Zhu, G., Klee, C. B. and Bax, A. (1992) Solution structure of a calmodulin-target peptide complex by multidimensional NMR. *Science* **256**, 632–638.

10 Gagne, S. M., Tsuda, S., Li, M. X., Smillie, L. B. and Sykes, B. D. (1995) Structures of the troponin C regulatory domains in the apo and calcium-saturated states. *Nat. Struct. Biol.* **2**, 784–789.

11 Strynadka, N. C., Cherney, M., Sielicki, A. R., Li, M. X., Smillie, L. B. and James, M. N. G. (1997) Structural details of a calcium-induced molecular switch: X-ray crystallographic analysis of the calcium-saturated N-terminal domain of troponin-C at 1.75 Å resolution. *J. Mol. Biol.* **273**, 238–255.

12 Donato, R. (2001) S100: a multigenic family of calcium-modulated proteins of the EF-hand type with intracellular and extracellular functional roles. *Int. J. Biochem. Cell Biol.* **33**, 637–668.

13 Odink, K., Cerletti, N., Bruggen, J., Clerc, R. G., Tarcsay, L., Zwadlo, G., Gerhards, G., Schlegel, R. and Sorg, C. (1987) Two calcium-binding proteins in infiltrate macrophages of rheumatoid arthritis. *Nature* (London) **330**, 80–82.

14 Van Eldik, L. J. and Griffin, W. S. T. (1994) S100b expression in Alzheimer's disease: relation to neuropathology in brain regions. *Biochim. Biophys. Acta* **1223**, 398–403.

S100 PROTEINS

The S100 proteins are small acidic proteins (10–12 kDa) that are found exclusively in vertebrates [15]. With at least 25 members found to date in humans, the S100 proteins constitute the largest subfamily of the EF-hand proteins. Of these, 21 family members (S100A1–S100A18, trichohylin, filaggrin and repetin) have genes clustered at chromosome locus 1q21, while other S100 proteins are found at chromosome loci 4p16 (S100P), 5q14 (S100Z), 21q22 (S100B) and Xp22 (S100G). First identified by Moore in 1965 [16], the S100 proteins have 25–65% identity at the amino acid level and contain two EF-hand motifs flanked by conserved hydrophobic residues and separated by a linker region [15]. The sequences of the linker region and the C-terminal extension are the most variable among the S100 proteins.

In addition to Ca^{2+} many S100 proteins display high affinities towards Zn^{2+} and Cu^{2+} ions, which could influence their activity in the extracellular space.

Three features are unique to the S100 proteins when compared with other EF-hand proteins. First, the two EF-hands in each monomer differ in sequence and mechanisms of calcium co-ordination. The 12-residue C-terminal EF-hand ligates calcium in a similar manner to calmodulin and troponin-C, resulting in a higher calcium affinity site with Kd10–50 mM [17]. The N-terminal or 'pseudo-canonical' EF-hand is formed by 14 residues and binds calcium mostly through main-chain carbonyl groups, except for the bidentate side chain of glutamate at the last position of the loop. This results in a weaker

15 Schafer, B. W. and Heizmann, C. W. (1996) The S100 family of EF-hand calcium-binding proteins: functions and pathology. *Trends Biochem. Sci.* **21**, 134–140.

16 Moore, B. W. (1965) A soluble protein characteristic of the nervous system. *Biochem. Biophys. Res. Commun.* **19**, 739–744.

17 Donato, R. (1986) S-100 proteins. *Cell Calcium* **7**, 123–145.

calcium affinity with Kd200–500 mM [17]. This presents an intriguing scenario for the S100 proteins in the cell whereby the C-terminal EF-hand has an affinity that would allow it to be populated during calcium influx, while the N-terminal site affinity is likely to be too weak to bind calcium at any appreciable level. The second unique characteristic of the S100 proteins is their dimeric nature. In vivo and in vitro experiments have shown that the S100 proteins can form non-covalent homo- and hetero-dimers. This indicates that dynamic exchange of the S100 subunits may occur, depending on the populations of the individual S100 protein members in a cellular compartment (**Figure 1**). Finally, S100 proteins are expressed in a tissue- and cell-specific fashion [12]. For example, S100A1 and S100A2 are found in the cytoplasm and nucleus respectively of smooth-muscle cells [18], whereas S100P is located in the cytoplasm of placental tissue [19, 20]. Together, this results in a complex picture of calcium signalling by the S100 proteins governed by the interchange of homo- and hetero-dimeric protein species, calcium binding to the proteins, interaction with target proteins, cell specificity and regulation of biological function (**Figure 1**).

S100 PROTEINS FUNCTIONS

The members of the S100 proteins family are multifunctional signalling proteins and are involved in the regulation of diverse cellular processes such as contraction, motility, cell growth, differentiation, cell cycle progression, transcription, and secretion. This variety

18 Mandinova, A., Atar, D., Schafer, B. W., Spiess, M., Aebi, U. and Heizmann, C. W. (1998) Distinct subcellular localization of calcium binding S100 proteins in human smooth muscle cells and their relocation in response to rises in intracellular calcium. *J. Cell Sci.* **111**, 2043–2054.

19 Emoto, Y., Kobayashi, R., Akatsuka, H. and Hidaka, H. (1992) Purification and characterization of a new member of the S-100 protein family from human placenta. *Biochem. Biophys. Res. Commun.* **182**, 1246–1253.

20 Becker, T., Gerke, V., Kube, E. and Weber, K. (1992) S100P, a novel Ca^{2+}-binding protein from human placenta. cDNA cloning, recombinant protein expression and Ca^{2+} binding properties. *Eur. J. Biochem.* **207**, 541–547.

of functions is reflected in broad diversification of the different members; e.g., in human there are 20 members that have 22% to 57% sequence identity, and vary between 79 and 114 amino acid residues in length. Further diversity is achieved by different metal ion-binding properties of the individual S100 proteins, by spatial distribution in specific intracellular compartments or in extracellular space, and by their ability to form homo- and heterodimers.

S100 proteins regulate different enzymes, Ca^{2+} homeostasis, cytoskeletal organization, and transcription in a Ca^{2+}-dependent manner. Detailed information is available in recent reviews [16, 17, 18, 19, 20]. At least one S100 protein, S100A10, interacts independently of Ca^{2+} with its target molecule annexin II. The EF-hands of S100A10 carry mutations rendering this S100 protein unable to bind Ca^{2+}. However, these mutations induce a protein conformation that resembles the Ca^{2+}-loaded state of S100A11, turning S100A10 into a constitutively active annexin-binding protein [10].

Many S100 proteins bind Zn^{2+} besides Ca^{2+} with high affinity. However, most of the reported Zn^{2+} dissociation constants are in the micromolar range versus nanomolar concentrations of free Zn^{2+} (1 to 5 nM) in the cytoplasm. Because of this low intracellular concentration, binding of Zn^{2+} to most S100 proteins in the cytoplasm is rather unlikely, as shown for S100B and S100A6 [15]. However, intracellular Zn^{2+} binding might occur in some vesicles that contain Zn^{2+} in micromolar to millimolar concentrations or in the extracellular space where the Zn^{2+} concentration is in the micromolar range [21]. An

21 Dempsey, A. C., Walsh, M. P. and Shaw, G. S. (2003) Unmasking the annexin I interaction from the structure of Apo-S100A11. *Structure* **11**, 887–897.

example of a Ca^{2+}-independent but Zn^{2+}-dependent target protein recognition is the interaction of S100B with tau protein [22].

S100 proteins have attracted increased attention in recent years owing to their cell- and tissue-specific expression and their involvement in several human diseases such as cystic fibrosis, rheumatoid arthritis, acute inflammatory lesions and acute myocardial ischemia [23, 24, 25, 26]. Another important aspect of the S100 family is that most of their genes are located in a gene cluster on human chromosome 1q21, which is structurally conserved in evolution. Within this chromosomal region, several gene rearrangements during tumor development have been described [27]. Indeed, some S100 proteins are involved in metastasis and cancer development [28].

S100A13

Among all the members reported in the S100 calcium-binding protein family, S100A13 is the only member that exhibits a ubiquitous expression in a broad range of tissues [23]. S100A13 is one of the latest member of the S100 family and was originally

22 Drohat, A. C., Tjandra, N., Baldisseri, D. M. and Weber, D. J. (1999) The use of dipolar couplings for determining the solution structure of rat apo-S100B(ββ). *Protein Sci.* **8**, 800–809.

23 Ridinger, K., Schafer, B. W., Durussel, I., Cox, J. A. and Heizmann, C. W. (2000). S100A13. Biochemical characterization and subcellular localization in different cell lines. *J. Biol. Chem.* **275**,8686 -8694.

24 Heizmann, C. W. and Cox, J. A. (1998). New perspectives on S100 proteins: a multi-functional Ca^{2+}-, Zn^{2+}- and Cu^{2+}-binding protein family. *Biometals* **11**,383 -397.

25 Donato, R. (2001). S100: a multigenic family of calcium-modulated proteins of the EF-hand type with intracellular and extracellular functional roles. *Int. J. Biochem. Cell Biol.* **33**,637 -668.

26 Heizmann, C. W., Fritz, G. and Schäfer, B. W. (2002). S100 proteins: structure, functions and pathology. *Frontiers Biosci.* **7**,D1356 -D1368.

27 Schäfer, B. W., Wicki, R., Engelkamp, D., Mattei, M. G. and Heizmann, C. W. (1995). Isolation of a YAC clone covering a cluster of nine S100 genes on human chromosome 1q21: rationale for a new nomenclature of the S100 calcium- binding protein family. *Genomics* **25**,638 -643.

28 Nagy, N., Brenner, C., Markadieu, N., Chaboteaux, C., Camby, I., Schafer, B. W., Pochet, R., Heizmann, C. W., Salmon, I., Kiss, R. et al. (2001). S100A2, a putative tumor suppressor gene, regulates in vitro squamous cell carcinoma migration. *Lab. Invest.* **81**,599 -612.

identified by screening the EST database [29]. It is similar to most other S100 proteins — homodimeric S100A13 possesses two high- and two low-affinity sites for calcium [23]. However, it does not show a calcium-dependent exposure of the hydrophobic surface, which is essential for the interaction of S100 proteins with their target proteins. S100A13 is associated with the secretion of brain-derived fibroblast growth factor-1 (FGF-1) and p40-synaptotagmin in response to heat shock [30, 31]. In addition, the anti-allergic and anti-inflammatory drug amlexanox which binds to S100A12 and S100A13, represses the secretion of FGF-1, S100A13 and p40-synaptotagmin 1 multi-aggregates [32, 33]. Therefore, S100A13 was postulated to play an important role in the release of FGF-1, as the growth factor lacks a classical signal sequence for secretion.

Calcium plays an important role as a second messenger in various signalling pathways. A sudden increase in the intracellular calcium level alters physiological cellular functions such as cell cycle progression, differentiation and muscle contraction [15]. One of the most commonly used factors to increase the intracellular calcium levels is angiotensin II. Angiotensin II is a potent smooth muscle constrictor, which increases cytosolic calcium

29 Wicki, R., Schafer, B. W., Erne, P. and Heizmann, C. W. (1996). Characterization of the human and mouse cDNAs coding for S100A13, a new member of the S100 protein family. *Biochem. Biophys. Res. Commun.* **227**,594 -599.

30 Jackson, A., Friedman, S., Zhan, X., Engleka, K. A., Forough, R. and Maciag, T. (1992). Heat shock induces the release of fibroblast growth factor 1 from NIH 3T3 cells. *Proc. Natl. Acad. Sci. USA* **89**,10691 -10695.

31 Landriscina, M., Soldi, R., Bagala, C., Micucci, I., Bellum, S., Tarantini, F., Prudovsky, I. and Maciag, T. (2001). S100A13 participates in the release of fibroblast growth factor 1 in response to heat shock in vitro. *J. Biol. Chem.* **276**,22544 -22552.

32 Carreira, C. M., LaVallee, T. M., Tarantini, F., Jackson, A., Lathrop, J. T., Hampton, B., Burgess, W. H. and Maciag, T. (1998). S100A13 is involved in the regulation of fibroblast growth factor-1 and p40 synaptotagmin-1 release in vitro. *J. Biol. Chem.* **273**,22224 -22231.

33 Shishibori, T., Oyama, Y., Matsushita, O., Yamashita, K., Furuichi, H., Okabe, A., Maeta, H., Hata, Y. and Kobayashi, R. (1999). Three distinct anti-allergic drugs, amlexanox, cromolyn and tranilast, bind to S100A12 and S100A13 of the S100 protein family. *Biochem. J.*

levels by interacting with angiotensin receptors [34, 35, 36, 37, 38]. Through a GTP-binding protein, angiotensin II activates phospholipase C, which generates inositol 1,4,5-trisphosphate (Ins(1,4,5)P3) and releases calcium from intracellular stores [39].

Translocation involves protein relocation to different intracellular compartments, and it has been implicated in association with signal transduction cascades. Protein translocation in response to intracellular calcium change has long been observed with protein kinase C (PKC) [40, 41, 42] and recently with some S100 proteins [43, 44, 45, 46]. S100A8 and S100A9 show calcium-dependent translocation in mye-lomonocytic cells and

34 Schiffrin, E. L. (1998). Vascular protection with newer antihypertensive agents. *J. Hypertens. Suppl.* **16**,S25 -S29.

35 Watts, S. W., Florian, J. A. and Monroe, K. M. (1998). Dissociation of angiotensin II-stimulated activation of mitogen- activated protein kinase kinase from vascular contraction. *J. Pharmacol. Exp. Ther.* **286**,1431 -1438.

36 Purdy, K. E. and Arendshorst, W. J. (1999). Prostaglandins buffer ANG II-mediated increases in cytosolic calcium in preglomerular VSMC. *Am. J. Physiol.* **277**,F850 -F858.

37 Takeuchi, K. (1999). Signal transduction systems of angiotensin II receptors *Nippon Rinsho.* **57**,1070 -1077.

38 Rossier, M. F. and Capponi, A. M. (2000). Angiotensin II and calcium channels. *Vitam. Horm.* **60**,229 -284.

39 Marks, A. R. (1992). Calcium channels expressed in vascular smooth muscle. *Circulation* **86 (6 Suppl.)**,III61 -67.

40 Damron, D. S., Nadim, H. S., Hong, S. J., Darvish, A. and Murray, P. A. (1998). Intracellular translocation of PKC isoforms in canine pulmonary artery smooth muscle cells by ANG II. *Am. J. Physiol.* **274**,L278 -L288.

41 Oancea, E. and Meyer, T. (1998). Protein kinase C as a molecular machine for decoding calcium and diacylglycerol signals. *Cell* **95**,307 -318.

42 Marsigliante, S., Muscella, A., Greco, S., Elia, M. G., Vilella, S. and Storelli, C. (2001). Na+/K+ATPase activity inhibition and isoform-specific translocation of protein kinase C following angiotensin II administration in isolated eel enterocytes. *J. Endocrinol.* **168**,339 -346.

43 Goebeler, M., Roth, J., van den Bos, C., Ader, G. and Sorg, C. (1995). Increase of calcium levels in epithelial cells induces translocation of calcium-binding proteins migration inhibitory factor-related protein 8 (MRP8) and MRP14 to keratin intermediate filaments. *Biochem. J.* **309**,419 -424.

44 Guignard, F., Mauel, J. and Markert, M. (1996). Phosphorylation of myeloid-related proteins MRP-14 and MRP-8 during human neutrophil activation. *Eur. J. Biochem.* **241**,265 -271.

45 van den Bos, C., Roth, J., Koch, H. G., Hartmann, M. and Sorg, C. (1996). Phosphorylation of MRP14, an S100 protein expressed during monocytic differentiation, modulates Ca(2+)-dependent translocation from cytoplasm to membranes and cytoskeleton. *J. Immunol.* **156**,1247 -1254

46 Brett, W., Mandinova, A., Remppis, A., Sauder, U., Ruter, F., Heizmann, C. W., Aebi, U. and Zerkowski, H. R. (2001). Translocation of S100A1. *Biochem. Biophys. Res. Commun.* **284**,698 -703

in epithelial cells [43, 45]. S100A2, S100A4 and S100A6 translocate in response to ionophore A23187, cyclic ADP-ribose and thapsigargin in some tumor cells [47], and translocation of S100A11 and S100B has been described in human glioblastoma cell lines [48, 49]. Since S100 pro-teins lack the classical signal sequence for secretion, it is of great interest to investigate the translocation pathways of this group of proteins. Novel pathways such as tubulin-filament-dependent translocation have been reported in secretion and translocation of S100A8, S100A9 and S100A11 [50].

We report here the structural effects of CaII and CuII binding to S100A13 and show that binding of two CaII ions per monomer triggers key conformational changes leading the creation of two identical and symmetrical CuII-binding sites on the surface of the protein, close to the interface between the two monomers. This copper(II) binding site is unique among the S100 which are reported to bind CuII or ZnII, in addition to calcium ions. The opening up of the interhelical angle α3-α4 and the uncovering of H48 in Ca2-S100A13 facilitate CuII binding at a site bridging the N-terminus of one monomer with the hinge of the other monomer suggesting that CuII binding may trigger the interaction with the biological partners.

47 Mueller, A., Bachi, T., Hochli, M., Schäfer, B. W. and Heizmann, C. W. (1999). Subcellular distribution of S100 proteins in tumor cells and their relocation in response to calcium activation. *Histochem. Cell Biol.* **111**,453 -459

48 Davey, G. E., Murmann, P. and Heizmann, C. W. (2001). Intracellular Ca^{2+} and Zn^{2+} levels regulate the alternative, cell density-dependent secretion of S100B in human glioblastoma cells. *J. Biol. Chem.* **276**,30819 -30826.

49 Davey, G. E., Murmann, P., Hoechli, M., Tanaka, T. and Heizmann, C. W. (2000). Calcium-dependent translocation of S100A11 requires tubulin filaments. *Biochim. Biophys. Acta* **1498**,220 -232.

50 Rammes, A., Roth, J., Goebeler, M., Klempt, M., Hartmann, M. and Sorg, C. (1997). Myeloid-related protein (MRP) 8 and MRP14, calcium-binding proteins of the S100 family, are secreted by activated monocytes via a novel, tubulin-dependent pathway. *J. Biol. Chem.* **272**,9496 -9502

CONCLUSIONS

The NMR structure of S100A13 in the apo and CaII-bound states, which are in the dimeric state, reveals key conformational changes, which include helix reorientation and surface accessibility changes, leading to an optimal ligand arrangement for the creation of a type II CuII-binding site in each molecule of the dimer, which are here characterized through EPR and NMR spectroscopy. The CuII binding site is located in a completely different region from that found for ZnII and CuII in other proteins of the same family. The CuII sites lie on the surface of the protein close to the dimer interface, bridging the negatively charged N-terminal helix of one monomer and a hinge region of the other monomer.

In conclusion the present ^{15}N and ^{13}C NMR characterization has shown that CaII binding to S100A13 triggers sizable conformational changes thus creating a novel binding site for CuII on a solvent exposed location, suggesting that CuII binding may provide a mechanism for finetuning of the multiprotein complex which involves S100A13.

§ 1.2 INTERACTION OF THE TWO SOLUBLE METAL-BINDING DOMAINS OF YEAST CCC2 WITH COPPER(I)-ATX1

THE ROLE OF COPPER IN BIOLOGICAL SYSTEMS

Copper is a relevant metal presents as co-factors in many proteins. Biological systems did not utilize copper before the advent of atmospheric oxygen [51]. In the prevailing reducing conditions before this event, copper was in the water-insoluble Cu(I) state, in the form of highly insoluble sulfides, and was not available for biological processes. Cyanobacteria are thought to be responsible for the beginning of dioxygen production about 10^9 years ago. The appearance of a significant O_2 concentration in the atmosphere required another 200–300 million years because the oxygen produced was initially consumed by the oxidation of ferrous iron in the oceans. The advent of oxygen was a catastrophic event for most living organisms and irreversibly changed life on earth. In contrast to the oxidation of iron and its loss of bioavailability as insoluble Fe(III), the oxidation of insoluble Cu(I) led to soluble Cu(II). Biology also discovered that whereas enzymes involved in anaerobic metabolism were designed to operate in the lower portion of the redox spectrum, the arrival of dioxygen created the need for a new redox active metal which could attain higher redox potentials. Copper, now bioavailable, was ideally suited to exploit the oxidizing power of dioxygen. Copper began to be used in energy-capture systems like cytochrome *c* oxidase. The arrival of copper also coincided with the

51 O'Halloran, T.V. & Culotta, V.C. (2000) *J.Biol.Chem.* **275**, 25057-25060.

development of multicellular organisms which had extracellular cross-linked matrices capable of resisting attack by oxygen free radicals [51].

Copper proteins mainly have two functions, electron transfer and dioxygen transport and activation [51]. Copper ion have, indeed, an unique chemistry due to its ability to adopt two distinct redox states, either oxidized as Cu(II) or in the reduced state, Cu(I). The Cu(II) has a $3d^9$ electronic conFiguretion and favors coordination numbers 4 (square planar), 5 (trigonal bypyramidal or square pyramid) or 6. The stable Cu(II)–N bonds are often inert while the bonds with oxygen donor ligands are more labile. Cu(I) is a closed shell d^{10} transition metal, prefers coordination number 2, 3 or 4(tetrahedral geometry) and is stabilized by soft ligands. Almost all of the copper proteins are extracellular; exceptions are cytochrome *c* oxidase, which is bound to the external face of the inner mitochondrial membrane and the copper-zinc superoxide dismutase found in the cytosol of eukaryotic cells. Type I copper proteins (blue copper proteins) have a highly covalent mononuclear Cu(II) center and catalyse electron transfers (plastocyanin, azurin). Type II copper proteins are mononuclear proteins which catalyse redox reactions (Cu_2Zn_2SOD, galactose oxidase, amine oxidase, Cu_B in cytochrome *c* oxidase). Type III copper proteins are binuclear, EPR silent in the oxidized Cu(II)-Cu(II) state. They participate in dioxygen transport (hemocyanin), dioxygen activation and oxygenation reactions (tyrosinase).

Previously, it was thought that metal enzymes captured their essential cofactor by collision processes with free metal ions or metal complexes with low-molecular-weight ligands. The mechanisms how metals are transported and inserted into diverse protein location is an emerging field in the scientific world and is just in the last years unraveling

[52, 53]. Both eukaryotes and prokaryotes have evolved several mechanisms that ensure efficient metal homeostasis. From biochemical, inorganic, structural, and mechanistic studies a new family of soluble metal receptor, know as "metallochaperones", have been found to interact with metal ions and deliver them to several targets in the cell [53]. This proteins have the role to guide and/or insert a metal cofactor into the active site of a target enzyme. In this frame the case of copper represents the most studied example of metal homeostasis. It was indeed proved that essentially no free copper is available in the cytoplasm of eukaryotic cells [53] being the total cytoplasmatic free copper concentration less than 10^{-18} M [53]. This feature eliminates the possibility that weakly bound copper ions can diffuse freely in the cell until a physiologically important active site captures the metal as it was observed *in vitro* where many copper enzymes easily acquire their metal without an auxiliary protein. The biological reason why free copper is not present in the cell is due to its toxicity. Indeed, excessive tissue accumulation of redox-active transition metals, as copper, can be cytotoxic, in particular because perturbations in metal homeostasis result in an array of cellular disturbances characterized by oxidative stress and increased free radical production.

Oxidative stress, defined as the imbalance between biochemical processes leading to production of reactive oxygen species, causes molecular damage that can lead to a critical failure of biological functions and ultimately cell death. Moreover, under reducing conditions free copper can be reduced from Cu(II) to Cu(I) oxidation state and becomes much more toxic, possibly because Cu(I) can diffuse through the cytoplasmic membrane

52 Nobrega, M.P., Bandeira, S.C.B., Beers, J. & Tzagoloff, A. (2002) *J.Biol.Chem.* **277**, 40206-40211.
53 Glerum, D.M., Shtanko, A. & Tzagoloff, A. (1996) *J.Biol.Chem.* **271**, 14504-14509.

[53, 54]. In particular Cu(I) toxicity could occur via the production of hydroxyl radicals (OH·) in a Fenton-type reaction.

$$Cu^{+} + H_2O_2 \Leftrightarrow Cu^{2+} + OH^{-} + OH\cdot \qquad (1)$$

Therefore, intracellular copper concentrations need to be regulated and copper homeostasis depends on a series of membrane proteins and smaller soluble proteins (copper chaperones), which exchange copper with the membrane-bound copper-transporting enzymes or incorporate the copper directly into copper-dependent enzymes. The progresses in knowledge of the molecular basis of copper homeostasis have been catalyzed by the identification of the genes involved in two human disorders of copper transport, Menkes disease (MD), and Wilson disease [54, 55]. The former is a fatal X-linked copper deficiency disorder due to mutations affecting Menkes gene (*MNK*). Individuals affected by Menkes disease usually die in early childhood and have multiple abnormalities that can be related to deficiencies in cuproenzymes. Differently in the Wilson disease very high concentrations of copper are accumulated in the liver because the biliary excretion of the metal ion is defective. If this disease is not treated, death can result from liver failure. Moreover, some very interestingly findings have linked copper to some neurodegenerative diseases as Alzheimer's disease, Creutzfeldt-Jakob disease, Parkinson's disease and Amyotrophic Lateral Sclerosis disease [55, 56].

54 Tzagoloff, A., Capitanio, N., Nobrega, M.P. & Gatti, D. (1990) *EMBO J.* **9**, 2759-2764.
55 Schulze, M. & Rodel, G. (1988) *Mol Gen Genet* **211**, 492-498.
56 Tzagoloff, A. & Dieckmann, C.L. (1990) *Microbiol Rev* **54**, 211-225.

COPPER ROUTES IN YEAST

The yeast *Saccharomyces cerevisiae* is an extremely attractive eukaryotic model system due to the easiness with which it can be grown, the facility with which it can be submitted to the powerful techniques of molecular biology and the fact that its complete genome has been completely sequenced. Known pathways for the delivery of copper in yeast are depicted in **Figure 2.**

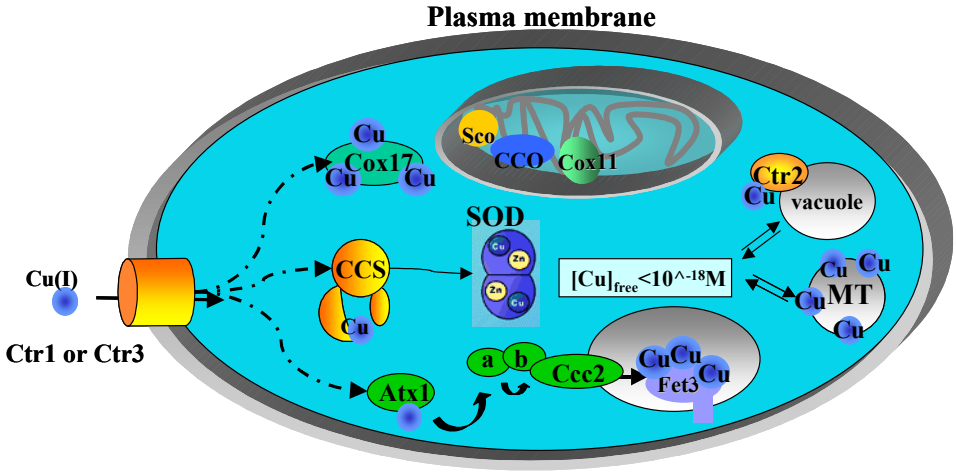

Figure 2

Copper transport and distribution in yeast.

Dashed arrows represent undefined pathways whereas solid arrows indicate established copper transfer pathways

Copper uptake, mediated by the cell surface copper transporters (Ctr), is deployed to mitochondrial cytochrome *c* oxidase, via a pathway involving Cox17, Sco and Cox11 proteins [57, 58], to cytosolic Cu_2Zn_2SOD, via a pathway involving a copper chaperone for

57 Dickinson, E.K., Adams, D.L., Schon, E.A. & Glerum, D.M. (2000) *J.Biol.Chem.* **275**, 26780-26785.

58 Hiser, L., Di Valentin, M., Hamer, A.G. & Hosler, J.P. (2000) *J.Biol.Chem.* **275**, 619-623.

SOD, called CCS [53, 59], or to the multicopper oxidase Fet3 in the secretory pathway involving the P-type ATPase copper transporter CCC2 [60] and the copper chaperone ATX1 [61, 62]. In addition cytosolic concentrations of free copper are typically maintained at low levels by metal scavenging systems like metallothioneins (MT) and by Ctr2 protein which is suggested to play a role in the mobilization of intracellular pools of copper in the vacuoles [63].

Ccc2 is a yeast homologue of the human copper(I)-transporting ATPases [64, 65]

At variance with ATP7A and ATP7B, Ccc2 does not traffic from the TGN to the plasma membrane, but is exclusively localized at the TGN membrane and thus only serves to transport copper from the cytosol into this organelle where the metal is incorporated in cuproenzymes. Ccc2 receives the copper(I) ions to be pumped across the membrane from a soluble metallochaperone, Atx1 (whose human counterpart is called HAH1 or Atox1). [66] (**Figure 3**).

59 Carr, H.S., George, G.N. & Winge, D.R. (2002) *J Biol Chem* **277**, 31273-31242.

60 Altschul, S.F., Madden, T.L., Schaeffer, A., Zhang, J., Zhang, Z., Miller, W. & Lipman, D.J. (1997) *Nucl.Acids Res.* **25**, 3389-3402.

61 Thompson, J.D., Higgins, D.G. & Gibson, T.J. (1994) *Nucl.Acids Res.* **22**, 4673-4680.

62 Hofmann, K. & Stoffel, W. (1993) *Biol.Chem.Hoppe-Seyler* **347**.

63 Tusnady, G.E. & Simon, I. (1998) *J Mol Biol* **283**, 489-506.

64 Yuan DS, Stearman R, Dancis A, Dunn T, Beeler T, Klausner RD. The Menkes/Wilson disease gene homologue in yeast provides copper to a ceru-loplasmin-like oxidase required for iron uptake. *Proc Natl Acad Sci U S A*. 1995 Mar 28; **92**(7):2632-6.

65 Odermatt A, Solioz M. Two trans-acting metalloregulatory proteins controlling expression of the copper-ATPases of Enterococcus hirae.b *J Biol Chem.* 1995 Mar 3; **270**(9):4349-54

66 Pufahl R., Singer C.P., Peariso K.L., Lin S.-J., Schmidt P.J., Fahrni C.J., Cizewski Culotta V., Penner-Hahn J.E., O'Halloran T.V. (1997) Metal ion chaperone function of the soluble Cu(I) receptor Atx1. *Science* **278**, 853-856.

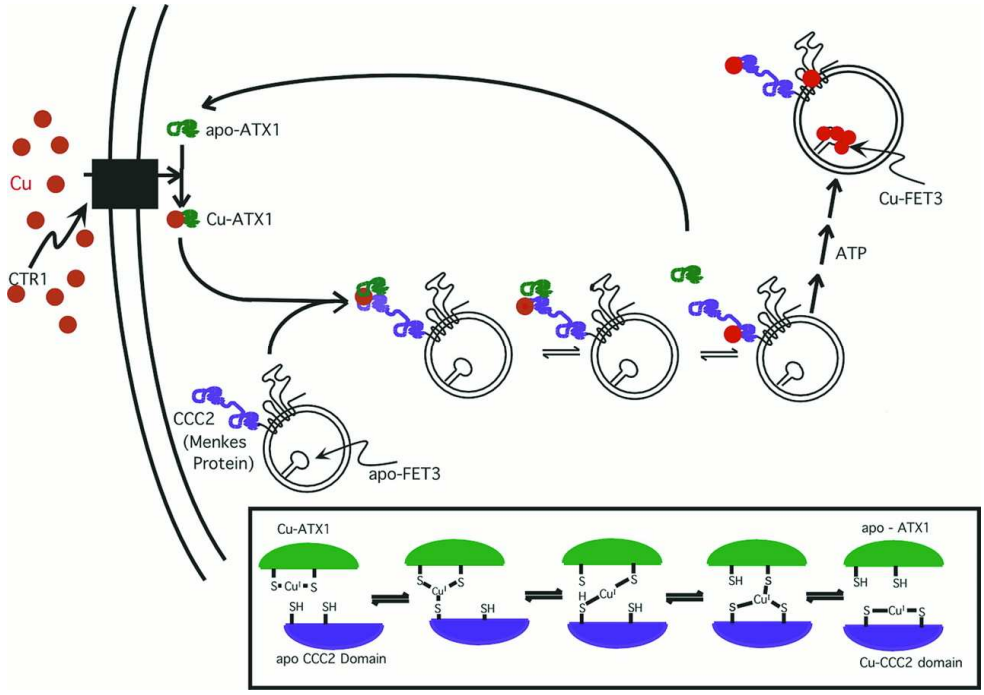

Figure 3

The copper trafficking pathway between Atx1 and the copper ATPases.

Copper destined for incorporation into the vesicular multicopper oxidase Fet3 requires both Ctr1 and Ccc2. Cu(I) (red spheres) is delivered via the metallochaperone Atx1 (green) to the N-terminal domains (purple) of the vesicular copper P-type ATPase Ccc2. In a step-wise mechanism, Cu(I)-Atx1 encounters Ccc2 and forms a transiently docked complex. Then copper rapidly equilibrates between the two domains. Concurrently, copper is pumped into the vesicle driven by the hydrolysis of ATP. In the vesicle, copper ultimately is incorporated into the multicopper oxidase Fet3. The human homologs of Atx1 (Hah1), Ccc2 (Menkes and Wilson proteins), and Fet3 (ceruloplasmin) are likely to employ similar mechanisms. (Inset) A proposed mechanism for the exchange of Cu(I) involving two- and three-coordinate Cu-bridged intermediates.

More in detail, Ccc2 is a multi-domain membrane protein, comprising a cytoplasmic region containing two distinct soluble metal-binding domains, which are quite similar in sequence to one another and are predicted to have the same fold (βαββαβ ferredoxin fold) as the partner protein Atx1. In both do-mains of Ccc2, as well as in Atx1, copper(I) is bound by two cysteines in a well conserved consensus sequence (MTCXXC)

located in a loop region[67, 68]. Various biochemical assays indicate that each of the two soluble metal-binding domains can interact with Atx1 [69, 70]. The structure of a copper-bridged adduct between the first metal-binding domain of Ccc2 (Ccc2a hereafter) and Atx1 has been solved using a combination of advanced NMR techniques and site-directed mutagenesis [69].

DIRECT COPPER TRANSFER BETWEEN YEAST ATX1 AND CCC2

Copper exchange rates in cysteines sites of proteins such as copper-metallothionein were generally thought to be slow due to the strength of the thiolate bonds [71]. In contrast, when the copper-bound form of the chaperone is directly incubated with apoCcc2a, Cu(I) equilibrates between the two proteins, and it does so rapidly [72], yielding an equilibrium constant (Equation 4, see below) of slightly greater than 1, $K_{exchange} = 1.4$. A step-wise mechanism for direct and rapid metal transfer is proposed in Equations 1–3.

67 van Dongen E.M., Klomp L.W., Merkx M. (2004) Copper-dependent protein-protein interactions studied by yeast two-hybrid analysis. *Biochem. Biophys. Res. Commun.* **323**, 789-795.

68 Morin I., Cuillel M., Lowe J., Crouzy S., Guillain F., Mintz E. (2005) Cd2+- or Hg2+-binding proteins can replace the Cu+-chaperone Atx1 in delivering Cu+ to the secretory pathway in yeast. *FEBS Lett.* **579**, 1117-1123.

69 Banci L., Bertini I., Cantini F., Felli I.C., Gonnelli L., Hadjiliadis N., Pierattelli R., Rosato A., Voulgaris P. (2006) The Atx1-Ccc2 complex is a metal-mediated protein-protein interaction. *Nat. Chem. Biol.* **2**, 367-368.

70 Kuhlbrandt W. (2004) Biology, structure and mechanism of P-type ATPases. Nat. Rev. Mol. Cell Biol. **5**, 282-295.

71 Fraústo da Silva JJR, Williams RJP. 1991. *The Biological Chemistry of the Elements*. New York: Clarendon. 561 pp.

72 Huffman DL, O'Halloran TV. 2000. *J. Biol. Chem.* **275**: 18611–14

$$K_1 \quad \text{Cu-Atx1} + \textit{apo}\text{Ccc2a} \underset{k_{-1}}{\overset{k_1}{\rightleftharpoons}} [\text{Cu-Atx1}/\textit{apo}\text{Ccc2a}] \qquad 1.$$

$$K_2 \quad [\text{Cu-Atx1}/\textit{apo}\text{Ccc2a}] \underset{k_{-2}}{\overset{k_2}{\rightleftharpoons}} [\textit{apo}\text{Atx1}/\text{Cu-Ccc2a}] \qquad 2.$$

$$K_3 \quad [\textit{apo}\text{Atx1}/\text{Cu-Ccc2a}] \underset{k_{-3}}{\overset{k_3}{\rightleftharpoons}} \textit{apo}\text{Atx1} + \text{Cu-Ccc2a} \qquad 3.$$

$$K_{\text{exchange}} \quad \text{Cu-Atx1} + \textit{apo}\text{Ccc2a} \underset{k_r}{\overset{k_f}{\rightleftharpoons}} \textit{apo}\text{Atx1} + \text{Cu-Ccc2a} \qquad 4.$$

In the first step (Equation 1), CuAtx1 transiently docks with *apo*Ccc2a. A specific orientation between CuAtx1 and *apo*Ccc2a could poise the Cu(I) center for nucleophilic attack by thiol from the adjacent protein, forming a Cu-$(S\text{-}Cys)_3$ intermediate. In the next step (Equation 2), the copper rapidly partitions between the two metal-binding sites within the protein-protein complex via formation and decay of two- and three-coordinate copper thiolate intermediates. In the final step (Equation 3), the complex dissociates to provide *apo*Atx1 and Cu-Ccc2a.

The relative rates and driving forces for individual steps are not yet established. However, given similarities in the copper-binding loops, we anticipate that K_2 will be approximately 1. In such a scenario, the equilibrium constant, K_1, for the encounter step could be significantly larger than 1, as long as the constant for the release step, K_3, is the reciprocal of K_1.

THERMODYNAMIC VERSUS KINETIC CONTROL OF COPPER TRAFFICKING

The metal-exchange results demonstrate that the thermodynamic gradient for copper transfer between this copper chaperone and its target domains is ~0.2 kcal/mol and is thus shallow ($K_{exchange}$ = 1.4 +/− 0.2). Thus, thermodynamics of vectorial copper delivery from the copper chaperone to targets involves small differences in the Cu(I)-binding constants of each protein or domain. If the subsequent Cu(I) transfer step to another site in Ccc2, such as the CXC motif [73], is rapid, then each of the copper transfer steps in **Figure 3** would be coupled with the driving force ultimately being provided by ATP hydrolysis. In the calcium P-type ATPases, the latter step induces a conformational change that translocates the cation across the membrane and into a thermodynamically separate compartment [74].

Since the initial Cu(I) transfer between Atx1 and Ccc2 proceeds rapidly to equilibrium, this step in the cellular trafficking pathway is best considered to be under thermodynamic control. However, Rae et al [75] have shown that intracellular free copper concentration is negligible, and they further suggest that the cytoplasm has a significant overcapacity for copper chelation. This leads to the dilemma of how the copper chaperone can retain Cu(I) in the face of a significant thermodynamic sink if transfer reactions are under thermodynamic control, but copper transfer from chaperone to target is not driven by thermodynamics of the copper-binding sites in these proteins. Rather, Atx1 appears to function as an enzyme: It lowers the kinetic barrier for copper transfer along specific

73 Solioz M, Vulpe C. 1996. *Trends Biochem. Sci.* **21**: 237– 41

74 Carafoli E. 1992. *J. Biol. Chem.* **267**: 2115– 18

75 Rae TD, Schmidt PJ, Pufahl RA, Culotta VC, O'Halloran TV. 1999. *Science* **284**: 805– 8

reaction coordinates. In this model, Atx1 catalyzes equilibration of copper between yet-to-be-identified copper donor sites and specific targets, such as Ccc2. ATP hydrolysis then drives the compartmentalization of the cytosolic copper available to Atx1. Finally, Atx1 may prevent adventitious copper release by deterring ligand exchange reactions with nonpartner proteins, although additional transfer reactions with the latter are required to test this.

AIM OF THIS WORK

A long-standing open question is the role of the multiple cytosolic metal-binding domains in copper-transporting ATPases. Homologous ATPases even from phylogenetically close organisms display a variable number of such do-mains, with different fold stability and different capability of binding copper [76]. The simplest systems (found in prokaryotes) contain only one such do-main. Yeast contains two domains. The honey bee, the fruit fly and the Caenorhabditis elegans worm have four domains. Humans and several other mammals instead contain as many as six domains, whereas the rhesus macaque (Macaca mulatta) only has five. Notably, other metal-transporting P-type ATPases such as the sarcoplasmic/endoplasmic reticulum calcium ATPase (SERCA) or the Na+/K+ ATPase do not possess any cytoplasmic metal-binding domain [77]. Various experiments based on the rescue of yeast variants where the ccc2 gene had been suppressed have shown that truncated variants of human ATP7A or ATP7B containing only two or even one

76 Arnesano F., Banci L., Bertini I., Ciofi-Baffoni S., Molteni E., Huffman D.L., O'Halloran T.V. (2002) Metallochaperones and metal transporting ATPases: a comparative analysis of sequences and structures. *Genome Res.* **12**, 255-271.

77 Lutsenko S, Kaplan JH. Organiza-tion of P-type ATPases: significance of structural diversity. *Biochemistry.* 1995 Dec 5; **34**(48):15607-13. Review

soluble domain allow Δccc2 yeast to grow on an iron- and copper-limited medium at levels close to that of wild-type yeast [78, 79, 80]. Another noteworthy feature is that in the ATPases containing multiple soluble metal-binding do-mains, the two closest in sequence to the transmembrane segments are most of-ten closely spaced in sequence (four to less than 10 aminoacids), whereas the other domains, if any, are widely spaced in sequence, with the linker stretches spanning up to several dozen aminoacids. The two domains closest to the C-terminus of the cytosolic copper(I)-binding region thus form a relatively com-pact unit, which is only loosely coupled, from a structural point of view, to the remainder of the tail. The organization of these two domains in the ATP7B protein prevents transfer of copper(I) from one domain to the other [81]. Based on these observations, it has been proposed that in the proteins containing more than two domains, the cellular role of the additional domains is that of regulat-ing protein trafficking between the TGN and the plasma membrane [79, 82, 83]. To obtain further insight into these complex systems, we have undertaken an NMR investigation of the entire two-domain cytoplasmic region of Ccc2 and of its interaction with copper(I) and with copper(I)-Atx1.

78 Payne A.S., Gitlin J.D. (1998) Functional expression of the Menkes disease protein reveals common biochemical mechanisms among the copper-transporting P-type ATPase. *J. Biol. Chem.* **273**, 3765-3770.

79 Cater M.A., Forbes J.R., La Fontaine S., Cox D., Mercer J.F. (2004) Intracellular trafficking of the human Wilson protein: the role of the six N-terminal metal-binding sites. *Biochem J.* **380**, 805-813.

80 Voskoboinik I., Strausak D., Greenough M., Brooks H., Petris M., Smith S., Mercer J.F., Camakaris J. (1999) Functional analysis of the N-terminal CXXC metal-binding motifs in the human menkes copper-transporting P-type ATPase expressed in cultured mammalian cells. *J. Biol. Chem.* **274**, 22008-22012.

81 Achila D., Banci L., Bertini I., Bunce J., Ciofi-Baffoni S., Huffman D.L. (2006) Structure of human Wilson protein domains 5 and 6 and their interplay with domain 4 and the copper chaperone HAH1 in copper uptake. *Proc. Natl. Acad. Sci. USA* **103**, 5729-5734.

82 Tsivkovskii R., MacArthur B.C., Lutsenko S. (2001) The Lys1010-Lys1325 fragment of the Wilson's disease protein binds nucleotides and interacts with the N-terminal domain of this protein in a copper-dependent manner. *J. Biol. Chem.* **276**, 2234-2242.

83 Banci L., Bertini I., Cantini F., Della Malva N., Migliardi M., Rosato A. The intermolecular interactions of the soluble copper-binding domains of the Menkes protein, ATP7A. *J.Biol.Chem.* 2007. Ref Type: In Press

CONCLUSIONS

Overall, the present data reinforce the view that the two copper(I)-binding domains that are closest to the transmembrane region are essentially two functionally independent units. In fact they can be independently metallated, they can independently interact with the physiological partner(s), they can have different features in terms of stability and dynamics.

The short linker separating the domains therefore may be important to prevent potential impairments in the uptake of the metal ion of each domain from the partner metallo-chaperone and/or in the delivery to the metal-binding site in the transmembrane region of the protein. This might be achieved by ensuring that the two domains cannot get one in the way of the other, providing steric restrictions along the copper(I)-transport pathway.

§ 1.3 STRUCTURE AND CU(I)-BINDING PROPERTIES OF THE N-TERMINAL SOLUBLE DOMAINS OF BACILLUS SUBTILIS COPA

COPPER ROUTES IN BACTERIA

Homologs of yeast copper proteins have also been discovered in other eukaryotes including *Arabidopsis thaliana*, *Caenorhabditis elegans*, mice, rats, sheep, and humans and in prokaryotes. The latter lack the intracellular compartmentalization that is typical of eukaryotes (cyanobacteria being a notable exception); thus organelle-specific carriers of metals such as COX17 may not be essential. In bacteria, for example, copper zinc superoxide dismutase (Cu_2Zn_2SOD) is a periplasmic enzyme in contrast with eukaryotes, where Cu_2Zn_2SOD is located in cytosol. Furthermore, bacteria do not express a prokaryotic homologue to CCS but still a homologue to ATX1 protein, called CopZ, is present. A general search for copper proteins showed that bacteria are very diversified and may develop alternative routes for copper homeostasis [76]. **Figure 4** show an example of copper distribution in two different bacteria.

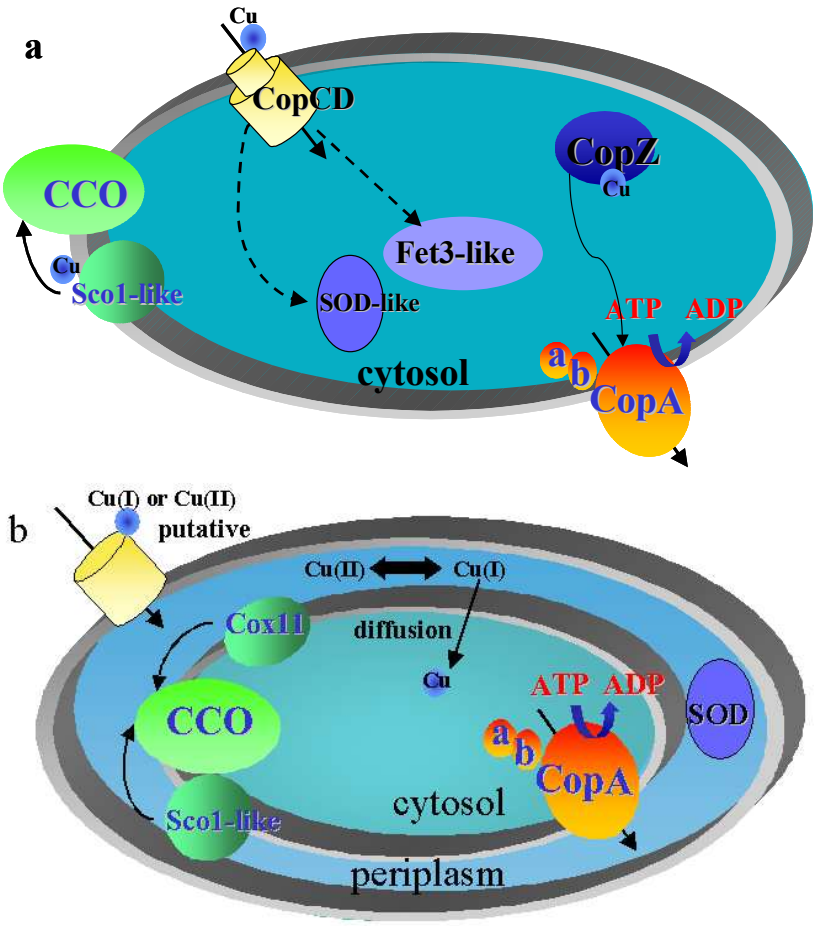

Figure 4 - Copper transport and distribution in *B. subtilis* (Gram-positive bacteria)**(a)** and in E. coli (Gram-negative bacteria)**(b)**. Dashed arrows represent undefined pathways whereas solid arrows indicate established copper transfer pathways

In this work we are interested in copper trafficking in *Bacillus subtilis*, the best characterised Gram-positive bacterium [84], which contains an Atx1-like copper chaperone, CopZ [85, 86], and a copper-transporting Ptype ATPase, CopA [87], which cooperate as

84 Sonenshein, A. L., Hoch, J., and Losick, R. (2001) Bacillus subtilis and its closest relatives: from genes to cells, *American Society for Microbiology*.

85 Banci, L., Bertini, I., Del Conte, R., Markey, J., and Ruiz-Duenas, F. J. (2001) Copper trafficking: The solution structure of *Bacillus subtilis* CopZ. *Biochemistry* **40**, 15660-15668.

part of a copper trafficking (export) pathway that is regulated in response to Cu(I) by the MerR-like protein CueR.

AIM OF THIS WORK AND CONCLUSION

CopA is a 803 amino acid residue protein with eight predicted transmembrane segments and two Nterminal soluble domains (approximately residues 1 – 72 and 73 – 147) that each contains a conserved MXCXXC metal binding motif typically found in homologous P-type ATPases and copper chaperone proteins [88]. These bear close resemblance in primary sequence to CopZ, and are involved in accepting Cu(I) from CopZ [89]. The solution structure of the second N-terminal domain of CopA (CopAb) was previously determined as a separate domain and as part of a two domain protein [87]. These revealed almost identical ferredoxin-like structures typical for this class of copper chaperone. CopAa, either separately or as part of CopAab, was previously found to be unstable [87], but could be stabilized through the introduction of a single substitution,

86 Banci, L., Bertini, I., Ciofi-Baffoni, S., Gonnelli, L., and Su, X. C. (2003) Structural basis for the function of the N-terminal domain of the ATPase CopA from *Bacillus subtilis*. *J. Biol. Chem.* **278**, 50506-50513.

87 Banci, L., Bertini, L., Ciofi-Baffoni, S., D'Onofrio, M., Gonnelli, L., Marhuenda-Egea, F. C., and Ruiz-Duenas, F. J. (2002) Solution structure of the N-terminal domain of a potential copper-translocating P-type ATPase from Bacillus subtilis in the apo and Cu(I) loaded states. *J. Mol. Biol.* **317**, 415-429.

88 Rosenzweig, A. C., and O'Halloran, T. V. (2000) Structure and chemistry of the copper chaperone proteins. *Curr. Opin. Chem. Biol.* **4**, 140-147.

89 Banci, L., Bertini, I., Ciofi-Baffoni, S., Del Conte, R., and Gonnelli, L. (2003) Understanding copper trafficking in bacteria: Interaction between the copper transport protein CopZ and the N-terminal domain of the copper ATPase CopA from *Bacillus subtilis*. *Biochemistry* **42**, 1939-1949.

Ser46Val, leading to structures of domain a, separately [90], and as part of CopAab, which also revealed a typical Atx1-like structure.

Here we have generated a wild-type form of B. subtilis CopAab that is sufficiently stable for structural analysis, and we report the solution structure of the apo-form of the protein, and a detailed spectroscopic and bioanalytical investigation of the Cu(I)-binding properties of the protein. Although the binding motifs of both domains are able to participate in Cu(I)-binding, above a level of 1 Cu(I) per protein the protein undergoes dimerization, generating a highly luminescent species indicative of the presence of a solvent-excluded multinuclear Cu(I) cluster.

Thus, it is an intriguing possibility that interactions between the N-terminal domains of different CopA molecules are mediated in response to Cu(I) levels and that this in turn influences the activity of the CopA efflux pump.

90 Banci, L., Bertini, I., Ciofi-Baffoni, S., Gonnelli, L., and Su, X. C. (2003) A core mutation affecting the folding properties of a soluble domain of the ATPase protein CopA from Bacillus subtilis. *J. Mol. Biol.* **331**, 473-484.

CHAPTER 2

METHODOLOGICAL ASPECTS

§ 2.1 NMR AND HIGH-RESOLUTION STRUCTURE DETERMINATION

X-ray crystallography and NMR spectroscopy are the two main techniques that can provide structures of macromolecules at atomic resolution. Both techniques are well established and play already a key role in structural biology as a basis for a detailed understanding of molecular functions. Whereas X-ray crystallography requires single crystals, NMR measurements are carried out in solution under conditions that can be as close as possible to the physiological state. Furthermore, the analysis through NMR spectroscopy easily allows the characterization under several, different experimental conditions, such as different ionic strength and pH. NMR measurements not only provide structural data but also can supply information on the internal mobility of proteins on various time scales, on protein folding and on intra-, as well as, intermolecular interactions.

The power of NMR technique respect the other spectroscopic techniques, results from the fact that each NMR active nucleus gives rise to an individual signal in the spectrum that can be resolved by multi-dimensional NMR techniques. This becomes more difficult for larger molecular structures (more than 50,000 Da) and puts a practical limit to the molecular size that can be studied in detail by NMR.

The principles of NMR structure determination can be summarized as follows:

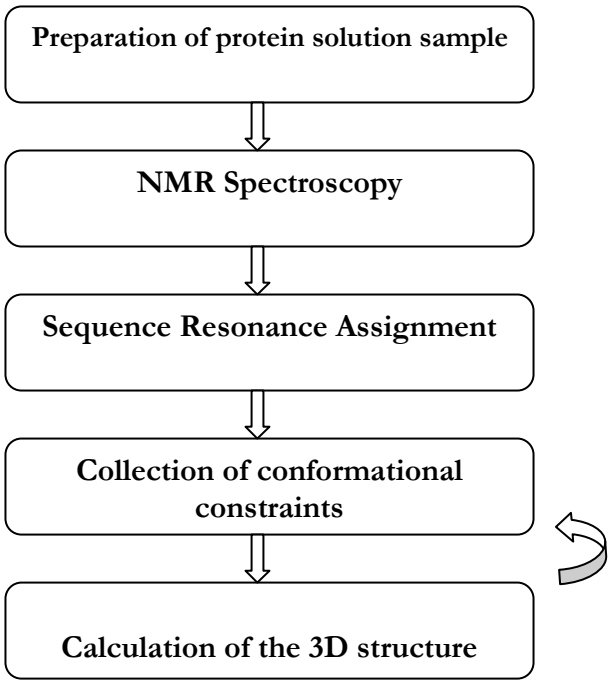

PREPARATION OF THE PROTEIN SOLUTION SAMPLE

The first step to solve the three dimensional structure of biological macromolecules is the preparation of the protein solution, since an highly purified protein preparation is required. An inhomogeneous preparation and/or aggregation of the protein as well as low molecular weight protonated impurities may severely harm the structure determination. The first step in every protein NMR study therefore involves optimization of the measurement conditions as pH, ionic strength, and temperature that can often be adjusted to mimic physiological conditions. The macromolecule under study should be stable in the chosen conditions for many weeks.

Proteins with a molecular weight larger than 10 kDa must be isotope enriched in ^{15}N and ^{13}C for an efficient structure determination. ^{15}N and ^{13}C are used because the most abundant carbon isotope (^{12}C) does not give a NMR signal and the most abundant nitrogen isotope (^{14}N) has undesired NMR properties.

NMR SPECTROSCOPY

NMR spectra of biological macromolecules contain hundreds or even thousands of resonance lines which cannot be resolved in a conventional one-dimensional spectra (1D). Further, the interpretation of NMR data requires correlations between different nuclei, which are implicitly contained in 1D spectra but often difficult to extract. Multidimensional NMR spectra provide both, increased resolution and correlations which are easy to analyse.

The crucial step in increasing the dimensionality of NMR experiments lies in the extension from one to two dimensions. A higher dimensional NMR experiment consists of a combination of two-dimensional (2D) experiments. All 2D NMR experiments use the same basic scheme which consists of the four following, consecutive time periods

excitation - evolution - mixing - detection

During the excitation period the spins are prepared in the desired state from which the chemical shifts of the individual nuclei are observed during the evolution period t1. In the mixing period the spins are correlated with each other and the information on the chemical shift of one nucleus ends up on an other nucleus of which the frequency is measured during the detection period t2. A resonance in the 2D spectrum, such as a cross peak, represents a pair of nuclei that suitably interact during the mixing time.

The extension from a 2D to a n-dimensional (nD) NMR experiment consists in the combination of (n-1) two-dimensional experiments which contains only one excitation and one detection period but repeats the evolution and mixing times (n-1) times. A typical nD NMR experiment thus follows the scheme:

$$\textbf{excitation - (evolution - mixing)}_{n-1}\textbf{ - detection}$$

where the bracket repeats (n–1) times. Only during the detection period the signal is physically measured and this period is often referred to as the direct dimension in contrast to the evolution periods which are referred to as indirect dimensions.

The NMR multidimensional measurements almost always use protons (^{1}H) and depending on the isotope labelling, ^{13}C and/or ^{15}N nuclei. A 3D spectrum can for example be obtained by correlating the amide groups with the α-carbon nuclei attached to ^{15}N. The chemical shifts of these carbon nuclei are used to spread the resonances from the 2D plane into a third dimension. The sensitivity obtainable with these types of nuclei greatly varies even if the sample is fully isotope labelled with ^{13}C or ^{15}N. The proton offers the best sensitivity and for this reason constitutes the preferred nucleus for detection of the NMR signal. The other nuclei are usually measured during evolution periods of multidimensional NMR experiments and their information is transferred to protons for detection.

For small proteins (less than 10kDa), it is not required to label the sample with ^{13}C or ^{15}N. In this case the assignment strategy makes use of a combination of 2D homonuclear ^{1}H NMR experiments such as COSY/TOCSY, and NOESY/ROESY spectra.

COSY- and TOCSY-type experiments, where COSY stands for *CO*rrelation *S*pectroscop*Y* and TOCSY for *To*tal *C*orrelation *S*pectrosco*py*, correlate different nuclei *via J* coupling. In proteins which are isotope labelled with ^{15}N and ^{13}C *J* couplings between ^{1}H, ^{15}N and ^{13}C allow *through-bond* correlations across the peptide bond.

Through-space correlations are instead measured via the nuclear Overhauser effect (NOE) and provide the basis for geometric information required to determine the structure of a macromolecule [91]. The NMR method for protein structure determination relies on a dense network of distance constraints derived from NOEs between nearby hydrogen atoms in the protein [92]. NOEs connect pairs of hydrogen atoms separated by less than about 5 Å. In contrast to COSY-type experiments the nuclei involved in the NOE correlation can belong to amino acid residues that may be far apart along the protein sequence but close in space. For molecules with a molecular weight of more than 5 kDa the intensity of an NOE is approximately proportional to r^{-6} and to the molecular weight, where *r* is the distance between the two interacting spins. NMR experiments which measure the NOE are often referred to as NOESY experiments where NOESY stands for *NOE S*pectroscop*Y* [93].

SEQUENCE RESONANCE ASSIGNMENT

For a detailed analysis of the information content of NMR spectra nearly complete assignments of signals in the spectra to individual atoms in the molecule are a requirement. The application of multidimensional NMR spectroscopy allowed the development of

91 Wider, G. (1998) *Progr.NMR Spectrosc.* **32**, 193-275.

92 , K. (1986) *NMR of Proteins and Nucleic Acids*, Wiley: New York

93 Kumar, A., Ernst, R.R. & Wüthrich, K. (1980) *Biochem.Biophys.Res.Commun.* **95**, 1104

general strategies for the assignment of signals in proteins. All procedures use the known protein sequence to connect nuclei of amino acid residues which are neighbours in the sequence. As mentioned before, for unlabelled proteins smaller than 10 kDa the combination of the [^{1}H,^{1}H]-COSY or TOCSY, used for the sequential assignment, with the [^{1}H, ^{1}H]-NOESY spectrum allows the assignment of most proton NMR signals to individual protons.

For larger proteins extensive signal overlap prevents complete assignments of all ^{1}H signals in proton spectra. This barrier can be overcome with 3D NMR technique and uniformly ^{13}C and ^{15}N labelled proteins. The resonance assignment of single (^{15}N or ^{13}C) labelled proteins using 3D experiments is basically an extension of Wüthrich's strategy which exclusively relies on homonuclear ^{1}H NMR experiments. With these methods, systems with molecular weights up to approximately 30 kDa can be studied.

In ^{13}C, ^{15}N-labeled proteins a sequential assignment strategy is based on through-bond correlations across the peptide-bond between sequential amino acids. This procedure circumvents the use of NOESY spectra already in the assignment step. Most of these correlation experiments use the three types of nuclei ^{1}H, ^{15}N, ^{13}C and are referred to as triple resonance experiments.

The 3D triple resonance experiments exclusively correlate the resonances of the peptide backbone (HN(i), N(i), Cα(i), Hα(i), Cα(i-1), CO(i) and CO(i-1)). **Figure 5** shows the spin system of the peptide backbone and indicates the size of the coupling constants used for magnetization transfer in double ^{13}C-, ^{15}N-labelled proteins. The 3D experiments used to identify the backbone resonances are, usually, HNCA or HNCACB, HN(CO)CA

or HN(CO)CACB, HNCO, HN(CA)CO and HNHA [94]. The HNCACB for example, correlates each H-^{15}N group with both the intra- and the neighbouring inter-residue Cα and and Cβ. These four types of connectivities are discriminated using the HN(CO)CACB experiment, in which only the inter-residue HN-Cα and Cβ couplings are observed.

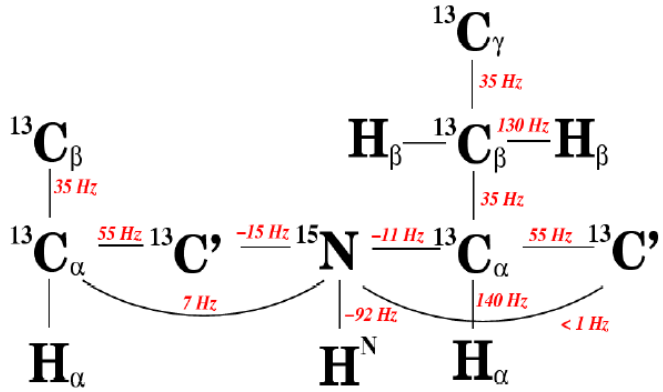

Figure 5 - Spin system of the peptide backbone and the size of the ^{1}J and ^{2}J coupling constants that are used for magnetization transfer in ^{13}C-, ^{15}N-labelled proteins.

Similar strategy can be used to assign the other resonances in the other triple resonance spectra.

In the case of proteins with a molecular weight larger than 30 kDa the use of TROSY-type experiments [95] is necessarily. TROSY experiment can reduce the signal loss, which is the direct consequence of the slower correlation tumbling of large molecules which results in faster relaxation and consequently broader lines in the NMR spectrum. TROSY uses constructive interference between different relaxation mechanisms and works

94 Kay, L.E., Ikura, M., Tschudin, R. & Bax, A. (1990) *J.Magn.Reson.* **89**, 496-514.
95 Pervushin, K. (2000) *Q.Rev.Biophys.* **33**, 161-197.

best at the highest available magnetic field strengths in the range of 700 to 900 MHz proton resonance frequency. With TROSY the molecular size of proteins accessible for detailed NMR investigations has been extended several fold. The TROSY technique benefits a variety of triple resonance NMR experiments as the 3D HNCA and HNCOCA [96] and the TROSY-based NOESY experiments for the collection of structural constraints are also available [97].

Since the Hα and Cα/β chemical shifts have been assigned, 3D H(C)CH-TOCSY and (H)CCH-TOCSY [98] experiments are then used to link the side chain spin systems to the backbone assignments. These two experiments provide information for the assignment of the side chain protons and of the side chain carbons, respectively.

A complete set of backbone chemical shifts for all Hα, Cα, Cβ and CO resonances can be used to predict the secondary structure of the protein [99]. One technique in particular, the Chemical Shift Index (CSI) [100], has been widely used for the quantitative identification and location of secondary structure in proteins.

The method relies on the fact that the chemical shifts of the different nuclei in the protein backbone are related both to the type of amino acid and to the nature of the secondary structure they are located in. By comparing the actual chemical shift for a nucleus in a specific amino acid with a reference value, it is possible to predict in what

96 Salzmann, M., Wider, G., Pervushin, K., Senn, H. & Wüthrich, K. (1999) *J.Am.Chem.Soc.* **121**, 844-848.

97 Pervushin, K.V., Wider, G., Riek, R. & Wuthrich, K. (1999) *Proc.Natl.Acad.Sci.USA* **96**, 9607-9612.

98 Kay, L.E., Xu, G.Y., Singer, A.U., Muhandiram, D.R. & Forman-Kay, J.D. (1993) *J.Magn.Reson.Ser.B* **101**, 333-337.

99 Wishart, D.S, Sykes, B.D. & Richards, F.M. (1991) *J.Mol.Biol.* **222**, 311-333.

100 Wishart, D.S., Sykes, B.D. & Richards, F.M. (1992) *Biochemistry* **31**, 1647-1651.

secondary structure element the nucleus resides. The reference value that you compare with is the random coil chemical shift for that same nucleus in the same amino acid.

COLLECTION OF CONFORMATIONAL CONSTRAINTS

For use in structure calculation, geometric conformational information in the form of distances and/or torsion angles has to be derived from the NMR data. The latter have to be supplemented by information about the covalent structure of the protein, such as the amino acid sequence, bond lengths, bond angles, chiralities, and planar groups, as well as by steric repulsion between non-bonded atom pairs.

Although a variety of NMR parameters contain structural information, the crucial information comes from NOE measurements which provide distance information between pairs of protons. Supplementary constraints can be derived from through bond correlations in the form of dihedral angles. Further, CSI data, provides, as before mentioned, information on the type of secondary structure. Such information can be included in a structure calculation by restricting the local conformation of a residue to the α–helical or β-sheet region of the Ramachandran plot through torsion angle restraints. Furthermore, hydrogen bonds can be experimentally detected via through-bond interactions [101] and they can be useful during structure calculations of larger proteins when not enough NOE data are available yet. Few years ago a new class of conformational restraints has been introduced that originates from residual dipolar couplings in partially aligned or paramagnetic molecules and gives information on angles between covalent bonds and

101 Cordier, F. & Grzesiek, S. (1999) *J.Am.Chem.Soc.* **121**, 1601-1602.

globally defined axes in the molecule, namely those of the magnetic susceptibility tensor [102, 103].

The intensity of a NOE, i.e. the volume V of the corresponding cross peak in a NOESY spectrum [104], is related to the distance r between the two interacting spins by:

$$V = \langle r^{-6} \rangle f(\tau_c) \qquad (1)$$

NOEs are usually treated as upper interatomic distance rather than as precise distance restraints. Adding the information on the distance between pairs of protons and their position in the polypeptide sequence allows construction of possible arrangements in which all distance constraints are fulfilled.

Of particularly utility for the NMR structure determination are scalar three-bond $^3J_{HX}$ coupling constants. The magnitude of these constants is related to dihedral angles subtended by the covalent bonds that connect the coupled nuclei H and X, where X can be ^1H, ^{15}N or ^{13}C. According to Karplus [105], the dependence of the three-bond J coupling constant on the dihedral angle θ subtended by the three successive covalent bonds that connect the coupled nuclei is embodied in the relation:

$$^3J(\theta) = A \cos^2(\theta) + B \cos(\theta) + C \qquad (2)$$

where θ = torsion angle (ϕ, φ, χ etc); A, B and C are Karplus constants depending on the type of the torsion angle. $^3J_{HNH\alpha}$ coupling constants (ϕ torsion angle) are obtained from the ratio between the intensity of the diagonal peak and that of the cross-peak of the HNHA map. Through the analysis of the HNHB spectrum the $^3J_{HNH\beta}$ coupling constants (χ torsion angles) can be derived. The process of defining useful conformational constraints on the basis of J coupling constants usually requires the translation of these quantities into molecular-geometry related dihedral-angle values.

102 Tolman, J.R., Flanagan, J.M., Kennedy, M.A. & Prestegard, J.H. (1995) *Proc.Natl.Acad.Sci.USA* **92**, 9279-9283.

103 Tjandra, N., Grzesiek, S. & Bax, A. (1996) *J.Am.Chem.Soc.* **118**, 6264-6272.

104 Macura, S. & Ernst, R.R. (1980) *Mol.Phys.* **41**, 95-95.

105 Karplus, M. (1963) *J.Am.Chem.Soc.* **85**, 2870-2871.

Using NMR constrains, calculation programs fold a random generated 3D structure, in order to maximize the agreement between the structure and the structural constrains. A NMR structure is represented by a family of conformers which are in good agreement with the structural constrains imposed. The precision of the structure is measured by the *root-mean-square-deviation* (RMSD) of the coordinates of the protein atoms for each conformer of the family from the mean structure and the accuracy of the structure is measured by an average *target function* of the family.

CHECK PROGRAMS

Programs have been developed to perform a `quality check' of a structure determined by X-ray crystallography or NMR spectroscopy. The best known examples of such programs are *procheck*, including its NMR-specific extension *procheck-nmr*, AQUA [106] and WHATIF [107]. These software packages try to assess the quality of a structure primarily by checking whether a number of different parameters are in agreement with their values in databases derived from high-resolution X-ray structures. Examples of such parameters include: correct values for covalent bond lengths and bond angles, the percentage of residues with ϕ/ψ values in the most favoured regions of the Ramachandran plot etc.

§ 2.2 ^{15}N RELAXATION IN PROTEINS

Protein mobility has an increasing relevance to our understanding of biological and chemical phenomena for the recognized importance of protein internal motions in biological processes. Macromolecular functions are often associated to energetic transition, which are intimately connected with structural changes and molecular flexibility.

106 Laskowski, R.A., Rullmann, J.A.C., MacArthur, M.W., Kaptein, R. & Thornton, J.M. (1996) *J.Biomol.NMR* **8**, 477-486.

107 Vriend, G. (1990) *J.Mol.Graphics* **8**, 52-56.

The measurement of ^{15}N relaxation rates in isotopically enriched proteins is particularly useful for obtaining dynamics information since the relaxation of this nucleus is governed predominantly by the dipolar interaction with directly bound proton and by the chemical shift anisotropy (CSA) mechanism.

In an ^{15}N relaxation experiment, one creates non-equilibrium spin order and records how this relaxes back to equilibrium. At equilibrium, the ^{15}N magnetization is aligned along the external field, and this alignment can be changed by radio frequency pulses. The magnetization will relax back to equilibrium along the direction of the magnetic filed with a constant time called longitudinal relaxation time T_1. When outside equilibrium the magnetization can have also a component perpendicular to the external magnetic field. The time constant for this spin component to return to equilibrium is called transverse relaxation time, T_2. A third source of relaxation parameter is the heteronuclear NOE. This is measured by saturating the proton (^1H) signal and observing changes in the ^{15}N signal intensities.

The relaxation parameters are related to the spectral density function, of the ^1H-^{15}N bond vector by the following equations [108].

$$T_1^{-1} = R_1 = (d^2/4)\left[J(\omega_H - \omega_N) + 3J(\omega_N) + 6J(\omega_H + \omega_N)\right] + c^2 J(\omega_N) \quad (3)$$

$$T_2^{-1} = R_2 = (d^2/8)\left[4J(0) + J(\omega_H - \omega_N) + 3J(\omega_N) + 6J(\omega_H) + 6J(\omega_H + \omega_N)\right] + (c^2/6)\left[4J(0) + 3J(\omega_N)\right] + R_{ex} \quad (4)$$

$$NOE = 1 + (d^2/4R_1)(\gamma_H/\gamma_N)\left[6J(\omega_H + \omega_N) - J(\omega_H - \omega_N)\right] \quad (5)$$

108 Abragam, A. (1961) *The Principles of Nuclear Magnetism*, Oxford University Press: Oxford

in which $d=(\mu_0 h\gamma_N\gamma_H/8\pi r^3_{NH})$ and $c=\omega_N\Delta_N/\sqrt{3}$. R_{ex} is a term introduced to account for microsecond to millisecond conformational exchange contributions to R_2.

The dynamic information contained in the relaxation rates are represented by the values of the spectral density function, $J(\omega)$, at several frequencies. The descriptions of the dynamics requires therefore the identification of a suitable model for the spectral density function, which must be consistent with the experimental relaxation rates. The spectral density is often expressed in terms of global tumbling parameters, and of local motional parameters.

SPECTRAL DENSITY MAPPING

The spectral density mapping approach was developed by Peng and Wagner in 1992 [109]. It makes use of six different relaxation parameters, which are used to map the spectral density function. These parameters are: 1) the longitudinal ^{15}N relaxation rate, R_1, 2) the transverse ^{15}N relaxation rate, R_2, 3) the $^1H\rightarrow^{15}N$ heteronuclear NOE, 4) the relaxation rate of longitudinal two-spin order $R_{NH}(2H_zN_z)$,5) the relaxation rate of anti-phase ^{15}N coherence $R_{NH}(2H_zN_{x,y})$ and 6) longitudinal relaxation of the amide protons.

The method of spectral density mapping does not require any assumption regarding the form of the spectral density functions. Values of the spectral density functions of ^1H-^{15}N vectors are directly sampled at several relevant frequencies (e.g. 0, ω_H-ω_N, ω_H+ω_N, ω_H, ω_N).

109 Peng, J.W. & Wagner, G. (1992) *J.Magn.Reson.* **98**, 308-332.

Drawbacks in this method reside in the fact that the three measurable relaxation parameters, R_1, R_2 and heteronuclear NOE, are insufficient to determine uniquely the values of the spectral density function at the five frequencies in equations (1) to (3) and that anomalous behaviour can be expected for the spectral densities at the three highest frequencies. These problems can be overcome by a more recent approach called reduced spectral density mapping, in which the values of the spectral density function at ω_H-ω_N, ω_H+ ω_N and ω_H frequencies can be combined in a average spectral density $<J(\omega_H)>$ [110, 111]. A comparison of $J(\omega)$ measured at high and low frequencies provides a quantitative measure of the breadth of the frequency distribution accessed through the spatial fluctuations of the bond and the overall tumbling of the molecule.

MODEL FREE APPROACH

A different method, called Model Free approach, has been introduced by Lipari and Szabo [112]. This model assumes that the overall rotation of the molecule can be described by a single correlation time (isotropic motion) and that this overall motion and the internal motions are independent. Then the total correlation function can be factored as:

$$C(t)= C_O(t)\times C_I(t) \qquad (6)$$

Where C(t) is the total correlation function, $C_O(t)$ is the correlation function characterizing the overall rotation and $C_I(t)$ is the correlation function characterizing the internal motions.

110 Farrow, N.A., Zhang, O., Szabo, A., Torchia, D.A. & Kay, L.E. (1995) *J.Biomol.NMR* **6**, 153-162.

111 Ishima, R. & Nagayama, K. (1995) *Biochemistry* **34**, 3162-3171.

112 Lipari, G. & Szabo, A. (1982) *J.Am.Chem.Soc.* **104**, 4546-4559.

As a consequence, the global spectral density function can be expressed as a weighted sum of Lorentzian functions. This is correct rigorously for isotropic rotational diffusion and approximately for anisotropic rotational diffusion.

The Lipari and Szabo formalism employs a minimum number of parameters to describe the overall isotropic tumbling motion of a macromolecule and the internal motions of the ^{15}N-^{1}H bond vector. The central equation in the Model Free Approach is:

$$J(\omega) = \left[\frac{S^2 \tau_m}{1 + (\omega \tau_m)^2} + \frac{(1 - S^2)\tau'}{1 + (\omega \tau')^2} \right] \qquad (7)$$

where τ_m is the correlation time as a result of the isotropic tumbling motion of the entire molecule. The effective correlation time resulting from internal motions is described by τ_e, where $\tau^{-1} = \tau_m^{-1} + \tau_e^{-1}$. The order parameter S^2 describes the degree of spatial restriction of the internal motion of the ^{1}H-^{15}N bond vector. It satisfies the inequality $0 \leq S \geq 1$ and lower values indicate larger amplitudes of internal motions. As a consequence, for a nucleus rotating as a whole with the molecule, all contributions to the spectral density function derive from the overall tumbling; alternatively, extra contributions will be described by other motions with correlation times faster than the overall tumbling.

An extended form of the model-free spectral density function has been developed by Clore and coworkers [113] to describe internal motions that take place on two distinct time scales, differing by at least an order of magnitude.

THE CONTRIBUTION TO RELAXATION OF EXCHANGE PROCESSES

The presence of exchange processes occurring in the micro-millisecond time scale produces dephasing of magnetization and contributes to make the transverse relaxation time shorter.

A method to obtain a detailed analysis of exchange contribution is the measurement of R_2 rates as a function of the refocusing times $\tau_{CPMG}(=1/(2\nu_{CPMG}))$, where ν_{CPMG} is the frequency of repetition of 180° pulses during the Carr-Purcell-Meiboom-Gill (CPMG) sequence [114]

The contribution of the exchange processes (R_{ex}) to the transverse relaxation rate can be expressed as follow [115]:

$$R_{ex} = \frac{k_{ex}}{2} - 2\nu_{eff} \sinh^{-1}\left(\frac{k_{ex}}{\xi}\sinh\frac{\xi}{4\nu_{eff}}\right) \qquad (6)$$

113 Clore, G.M., Szabo, A., Bax, A., Kay, L.E., Driscoll, P.C. & Gronenborn, A.M. (1990) *J.Am.Chem.Soc.* **112**, 4989-4991.

114 Mulder, F.A., Van Tilborg, P.J., Kaptein, R. & Boelens, R. (1999) *J.Biomol.NMR* **13**, 275-288.

115 Palmer, A.G., III, Williams, J. & McDermott, A. (1996) *J.Phys.Chem.* **100**, 13293-13310.

$$\text{where } \xi = (k_{ex}^2 - 4p_A p_B \delta\omega^2)^{1/2}, \; k_{ex} = 1/\tau_{ex} \text{ and } \nu_{eff}(s^{-1}) = \frac{1}{2(T_\pi + \tau_{CPMG})}$$

p_A and p_B are the populations of the sites A and B in a two-site exchange process, $\delta\omega$ is the difference of Larmor frequencies between the sites and τ_{ex} is the time constant for the exchange process.

CHAPTER 3

PUBBLICATIONS

Arnesano, F.; Banci, L.; Bertini, I.; Fantoni, A.; Tenori, L. and Viezzoli, M. S.; *Structural interplay between calcium(II) and copper(II) binding to S100A13*; Angew. Chem. Int. Ed., **39**, 6341-6344, 2005

Banci, L.; Bertini, I.; Chasapis, C.; Rosato, A. and Tenori, L.; *Interaction of the two soluble metal-binding domains of yeast Ccc2 with copper(I)-Atx1*; Biochem. Biophys. Res. Commun., 2007 Dec 21; **364**(3):645-9.

Singleton, C.; Banci, L.; Bertini, I.; Ciofi-Baffoni, S.; Tenori, L.; Kihlken, M. A.; Boetzel, R. and Le Brun, N. E.; *Structure and Cu(I)-binding properties of the N-terminal soluble domains of Bacillus subtilis CopA;* Biochemistry, submitted